RSC Advances

Journal Name

ARTICLE

High capacity and excellent rate capability of Ti-doped Li_2MnSiO_4 as cathode materials for Li-ion batteries

Min Wang [a], Meng Yang [a,*], Liqun Ma [a,*] Xiaodong Shen [a]

Ti-doped $Li_2Mn_{1-x}Ti_xSiO_4$ as cathode materials for Li-ion batteries was successfully synthesized by a facile sol-gel method. The addition of Ti to the precursors changed particle sizes and specific surface areas of Li_2MnSiO_4. The galvanostatic charge-discharge measurements showed that Ti-doped $Li_2Mn_{1-x}Ti_xSiO_4$ (x=0.06, 0.1, 0.2) electrodes delivered high charge capacity of 298, 286, 248 mAh g^{-1} and discharge capacity of 203, 211, 171 mAhg^{-1} in the first cycle, much higher than that of undoped Li_2MnSiO_4 (52 mAh g^{-1} for charging and 26 mAh g^{-1} for discharging). Moreover, Ti-doped samples exhibited good cycling stability and superior rate capability, as compared to that of pristine sample. Even at high rate (2C), the Ti-doped $Li_2Mn_{1-x}Ti_xSiO_4$ still kept high discharge capacities. The remarkable enhancement of battery performance in terms of capacity and rate capability for doped $Li_2Mn_{1-x}Ti_xSiO_4$ was primarily attributed to the decrease of charge transfer resistance and the improvement of Li^+ diffusion coefficient.

Introduction

Recently, Li_2MnSiO_4 as cathode materials for Li-ion batteries has attracted remarkable attention since first reported by R. Dominko et al.[1] in 2007. This material is expected to be the candidate cathode materials for next-generation rechargeable Li-ion batteries due to its high energy density, power density, high thermal stability, abundant resources, and environmentally friendly et al. [2-5] Most importantly, the transition metal manganese ion can easily achieve the transformation of Mn^{2+}/Mn^{3+} and Mn^{3+}/Mn^{4+} to carry out extraction of two Li^+, resulting high theoretical capacity of 330 mAh g^{-1}.[1,3] However, low intrinsic electronic conductivity and slow Li^+ mobility which cause excessive polarization during charge-discharge process, lead to low capacity and inferior electrochemical performance of this material.[6,7] Although carbon coating can improve electronic conductivity and reduce particle size which can shorten the pathway of Li^+ migration, Li_2MnSiO_4 still has large irreversible capacity loss and unsatisfactory cycling stability so that not sufficient for practical battery applications.[8,9] Thus, other feasible methods to enhance its battery performance should be found in urgent. Recently, few studies on ion doping of Li_2MnSiO_4 material have been reported. Zhang et al. [10] prepared Cr-doped Li_2MnSiO_4 with a citric acid-assisted sol–gel method. The obtained $Li_2Mn_{0.94}Cr_{0.06}SiO_4$ showed the best cycling performance and could deliver the discharge capacity of 306 mAh g^{-1} in the fifth cycle. Choi et al. [11] synthesized various ions (Al^{3+}, Ga^{3+}, Mg^{2+}) doped Li_2MnSiO_4 via the conventional sol-gel method. The sample doped with Ga^{3+} showed high charge/discharge

capacity and initial efficiency with well-dispersed nanoparticle formation. Hence, doping with metal ions might be a new strategy to improve the electrochemical performance of Li_2MnSiO_4 material.

Herein, we chose Ti element as doping cation for following reasons: 1) according to defect chemistry, aliovalent ion doping can induce defects (vacancies or interstitials) in the lattice by charge compensation so as to enhance the materials' conductivity.[11-14] 2) this element is inactive in the potential range of 1.5-4.8V, so the lattice shrinking of Li_2MnSiO_4 during charging is minimized by the support of unchangeable radius of Ti^{4+}.[10, 15]

In this paper, we successfully synthesized pristine Li_2MnSiO_4 and Ti-doped $Li_2Mn_{1-x}Ti_xSiO_4$ (x=0.06, 0.1 and 0.2) materials by a facile sol-gel method. The effects of Ti-doped Li_2MnSiO_4 materials in terms of structure, morphology and electrochemical properties have been investigated by X-ray diffraction (XRD), field emission scanning electron microscope (FE-SEM), inductively coupled plasma–atomic emission spectrometer (ICP-AES), Brunauer-Emmett-Teller (BET), galvanostatic charge-discharge and electrochemical impedance spectra (EIS) in details.

Experimental

Ti-doped $Li_2Mn_{1-x}Ti_xSiO_4$ (x=0.06, 0.1 and 0.2) powders were prepared by a facile sol-gel method. Analytical grade lithium acetate dihydrate, manganese acetate tetrahydrate, ethyl silicate and tetrabuty titanate were employed as raw materials. First, stoichimetric amounts of lithium acetate dihydrate and manganese

acetate tetrahydrate were dissolved in ethanol stirring for half an hour. Then, ethyl silicate in ethanol solution and tetrabuty titanate in ethanol solution was slowly added to above mixed solutions in order. The solutions were maintained at 80 ℃ for 24 hours under vigorously stirring and then dried in oven at 80 ℃ overnight. Subsequently, the obtained xerogel were fine ground by ball-milling and then calcined at 650℃ for 10 hours with a flow of argon. For comparison, undoped Li_2MnSiO_4 powder was prepared by identical process without adding tetrabuty titanate as the doping agent.

X-ray powder diffraction (XRD) was collected by diffractmeter (SmartLab, Japan) with Cu Kα (λ=1.5406 Å) radiation. The scanning angle 2θ was ranging from 10 to 80° at a step of 0.02°. The morphology and particle size distribution were observed by field emission scanning electron microscopy (FE-SEM, HITACHIS-4800, Japan). N_2 adsorption-desorption isotherms were measured by F-Sorb 2400 analyzer. The specific surface areas were calculated by using Brunauer-Emmett-Teller (BET) method. Chemical composition of all the samples were determined by inductively coupled plasma–atomic emission spectrometer (ICP-AES).

The electrochemical characterization of the materials was measured using a typical CR2032 coin cell. The working electrodes were prepared by mixing 80 wt. % active materials, 10 wt. % carbon black with 10 wt. % polyvinylidene fluoride (PVDF) via using 1-methyl-2-pyrrolidone as a solvent. Then, the resulting slurries were uniformly pasted on Al foils and dried in vacuum at 100 ℃ overnight. Circular electrodes were cut-off from the sheets with a diameter of 12 mm and the active materials ($Li_2Mn_{1-x}Ti_xSiO_4$) weights were maintained in the range of 1.9-2.1 mg cm^{-2}. The coin cells were assembled in a glove box filled with high pure argon(less than 1 ppm of water and oxygen) using Li metal as the anodes, celgard2400 film as the separator and 1 M $LiPF_6$ dissolved in EC and DMC (1:1 w/w) as the electrolyte. Meanwhile, galvanostatic charge–discharge measurements on (Land, China) were performed in the voltage range of 1.5-4.8 V (vs. Li^+/Li) under the current density of 10 mA g^{-1} at 30 ℃. Rate capability of electrodes was examined at various current densities: 0.03C, 0.1C, 0.5C, 1C, 2C (1C=330 mA g^{-1}). Electrochemical impedance spectra (EIS) were recorded by electrochemical workstation (CHI660D, China) in a frequency range from 10 mHz to 100 kHz with amplitude of 5 mV.

Results and Discussion

The typical powder X-ray diffraction (XRD) patterns of as-prepared pristine Li_2MnSiO_4 and Ti-doped $Li_2Mn_{1-x}Ti_xSiO_4$(x=0.06, 0.1 and 0.2) powders are shown in Fig.1. It can be seen that all the samples are well indexed to orthorhombic structure with $Pmn2_1$ space group, which is in accord with previous reports.[16,17] However, with the increasing of Ti content, some diffraction peaks identified as Mn_2TiO_4 and Li_2SiO_3 impurities are observed in the case of x=0.2, which are also reported by other researchers.[18-21] But neither of these impurities is considered for quantitative analysis, since they are electrochemically inactive in the voltage window of 1.5-4.8V [10]. In order to clarify the actual sites of dopants, Rietveld refinement is adopted. The refinements results are presented in Fig.2. We examine all the possible ways in which dopants occupy in the crystal lattice and the best fit results are obtained
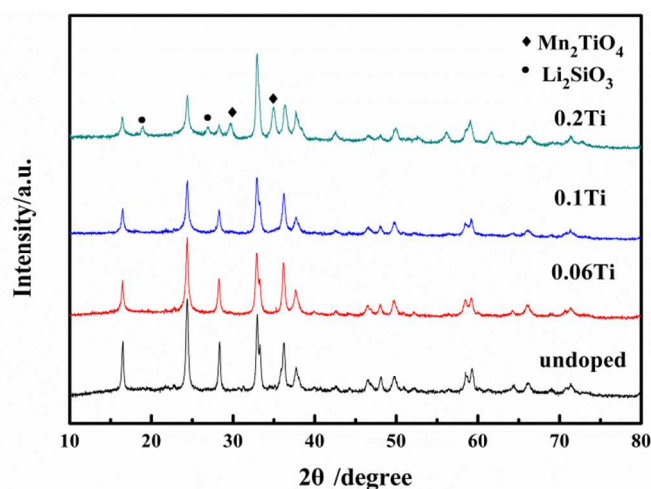
Fig.1 XRD patterns of as-prepared pristine Li_2MnSiO_4 and doped $Li_2Mn_{1-x}Ti_xSiO_4$(x=0.06, 0.1 and 0.2) powders

when Ti occupied Mn site. The reasonable values of Rp and Rwp can support this conclusion. The calculated lattice parameters of all these materials are listed in Table 1. Noting, doping Ti element induces the slight volume shrinkage of Li_2MnSiO_4, which might be ascribed to the smaller ionic radius of Ti^{4+} (0.68 Å) [22] than that of Mn^{2+} (0.80 Å), but the values of b-axis are a little enlargement. According to previous reports,[23,24] layers of SiO_4 and MnO_4 tetrahedral lying on the ac-plane link along the b-axis by LiO_4 tetrahedra, so enlargement of b values can expand the Li^+ diffusion channel to facilitate Li^+ mobility so as to enhance the electrochemical activity. The results of ICP-AES element analysis are demonstrated in Table 2, where the amount of element Mn is normalized to stoichiometry. As is seen, the actual compositions of all as-prepared powders are generally in line with nominal compositions.

FE-SEM images display the morphology of pristine and Ti-doped samples, as shown in Fig.3a-d. We can see that pristine Li_2MnSiO_4 powders exhibit severe agglomeration by nanosized
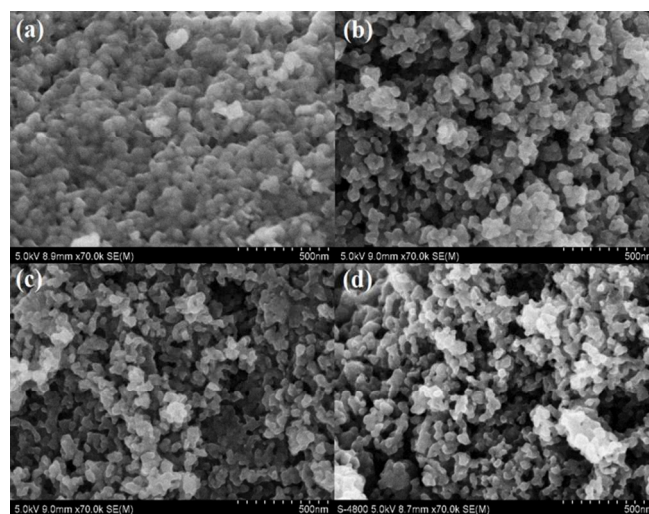
Fig.3 FE-SEM images of as-prepared $Li_2Mn_{1-x}Ti_xSiO_4$ powders: (a) x=0; (b) x=0.06; (c) x=0.1; (d) x=0.2
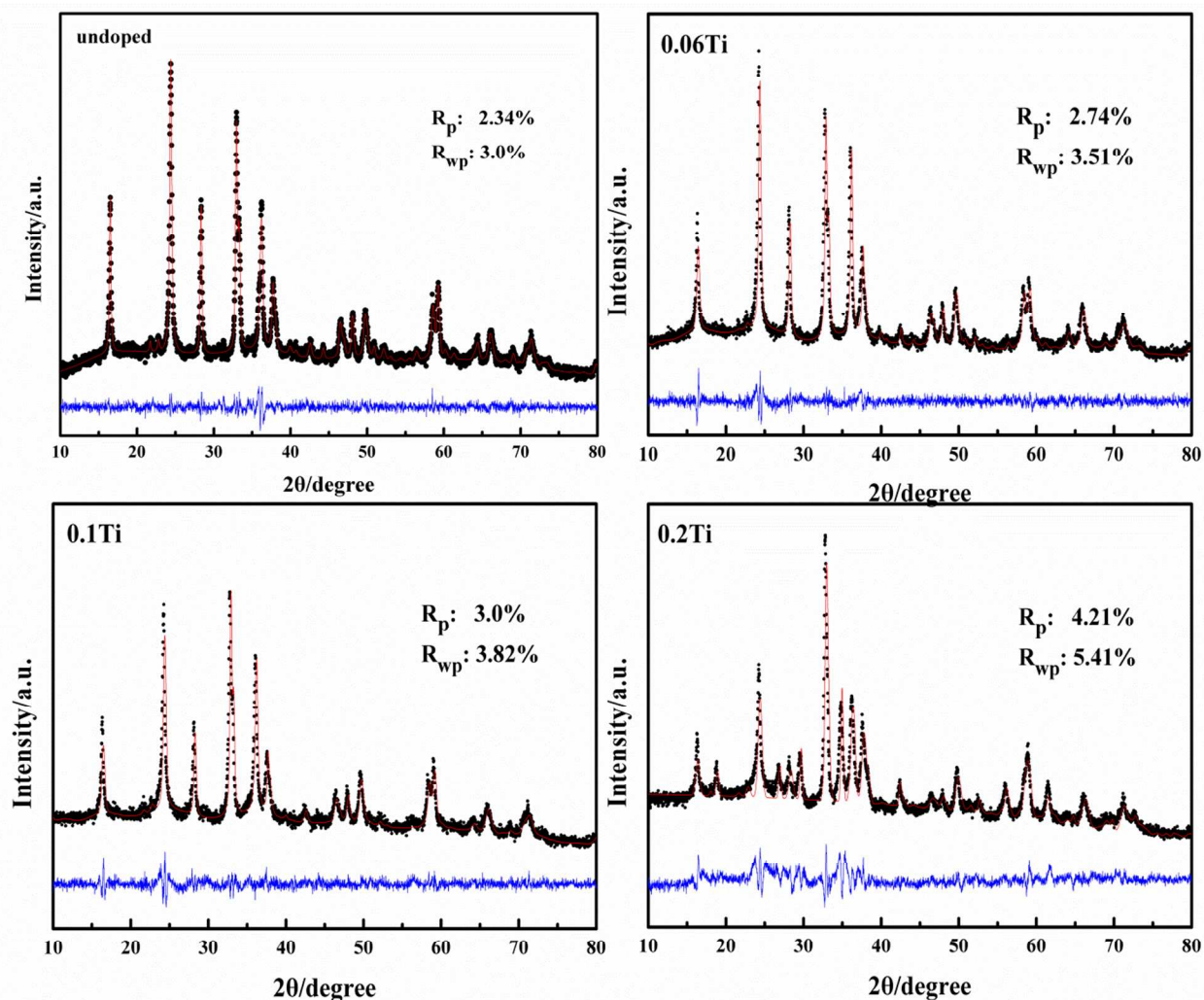
Fig.2 Refinement results of as-prepared $Li_2Mn_{1-x}Ti_xSiO_4$(x=0, 0.06, 0.1 and 0.2) powders.

Table 1 Lattice parameters and unit cell volumes of as-prepared $Li_2Mn_{1-x}Ti_xSiO_4$(x=0, 0.06, 0.1 and 0.2) samples

samples	a/Å	b/Å	c/Å	V/Å^3
Li_2MnSiO_4	6.3077	5.3884	4.9753	169.1025
$Li_2Mn_{0.94}Ti_{0.06}SiO_4$	6.3185	5.3908	4.9708	169.3142
$Li_2Mn_{0.9}Ti_{0.1}SiO_4$	6.3128	5.3913	4.9676	169.0683
$Li_2Mn_{0.8}Ti_{0.2}SiO_4$	6.2943	5.4117	4.9457	168.4647

Table 2 Chemical compositions of as-prepared $Li_2Mn_{1-x}Ti_xSiO_4$(x=0, 0.06, 0.1 and 0.2) samples obtained from ICP-AES, where the amounts of Mn are normalized

samples	Li	Mn	Ti
Li_2MnSiO_4	1.91	1.0	—
$Li_2Mn_{0.94}Ti_{0.06}SiO_4$	1.93	0.94	0.064
$Li_2Mn_{0.9}Ti_{0.1}SiO_4$	2.03	0.9	0.101
$Li_2Mn_{0.8}Ti_{0.2}SiO_4$	2.06	0.8	0.198
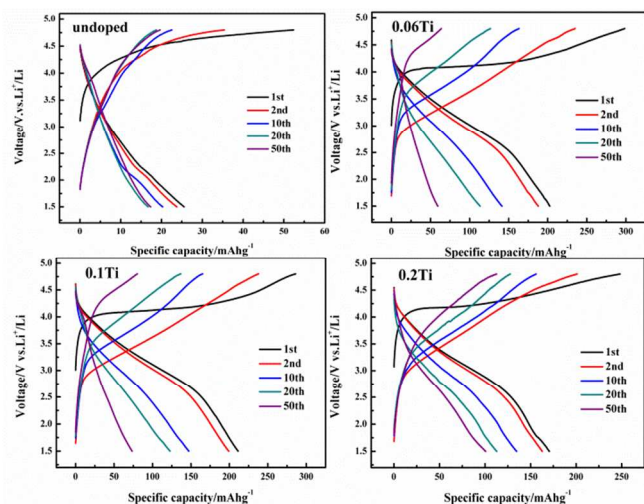
Fig.4 Charge-discharge curves of $Li_2Mn_{1-x}Ti_xSiO_4$(x=0, 0.06, 0.1 and 0.2) electrodes in different cycles

primary particles (~50 nm), while Ti-doped samples represent alleviative agglomeration between particles and the mean particle sizes are approximately 30 nm, much less than that of pristine sample. Moreover, the BET specific surface areas of $Li_2Mn_{1-x}Ti_xSiO_4$ are calculated to be 11.919 (x=0), 44.376 (x=0.06), 40.6 (x=0.1) and 35.197 (x=0.2) m^2g^{-1}, respectively. Obviously, doping Ti element can decrease the particle sizes, thus dramatically increasing the specific surface areas. The results can shorten the pathway of lithium-ion transfer and enable good contact between particles and the electrolyte so as to benefit the electrochemical reaction.

Additionally, the electrochemical performance of Ti-doped samples shows remarkable improvement, especially for capacity. For comparison, the charge-discharge curves of doped $Li_2Mn_{1-x}Ti_xSiO_4$ (x=0.06, 0.1 and 0.2) and pristine Li_2MnSiO_4 electrodes are presented in Fig.4, which were tested in a voltage range of 1.5-4.8V under a current density of 10 mA g^{-1} at 30 °C. It is clearly seen that pristine Li_2MnSiO_4 deliver extremely low capacity of 52 mAh g^{-1} for charging and 26 mAh g^{-1} for discharging in the first cycle, corresponding to 0.16 Li^+ and 0.08 Li^+ per formula unit, respectively. The poor electrochemical activity may be attributed to its low intrinsic electric conductivity ($<10^{-14}$ S cm^{-1} at RT).[1] However, in the case of Ti-doped $Li_2Mn_{1-x}Ti_xSiO_4$, all three samples demonstrate dramatically increased capacities. For x=0.06, 0.1 and 0.2, the capacities are 298, 286, 248 mAh g^{-1} for first charging(corresponding to 1.81, 1.73 and 1.50 Li^+ per formula unit) and 203, 211, 171 mAh g^{-1} for first discharging (corresponding to 1.23, 1.28 and 1.04 Li^+ per formula unit), respectively. Although the capacities decrease during prolonged cycle, they are still greatly improved, as compared to that of pristine Li_2MnSiO_4 electrodes. Among these Ti-doped samples, $Li_2Mn_{0.8}Ti_{0.2}SiO_4$ shows the best cycling stability, as shown in Fig.5. From 20th to 50th cycles, the capacity maintains around 100 mAh g^{-1} and it has a relatively high capacity retention rate of 60% after 50 cycles. As far as

we know, this should be the best result of Li_2MnSiO_4 electrodes without additional carbon coating so far.[25-27] The reasonable explanations of achieved high capacity and structural stability for doped $Li_2Mn_{1-x}Ti_xSiO_4$ electrodes are ascribed to ⅰ) according to the XRD results, for Ti-doped samples, the enlargement of Li^+ diffusion channel is beneficial to facilitate Li^+ mobility; ⅱ) decreased particle size and increased specific surface area can shorten the Li^+ migration pathway and enable good contact between particles and electrolyte so as to benefit the electrochemical reaction; ⅲ) Li_2MnSiO_4 is a typical n-type semiconductor, its electronic conduction takes place by electron hopping between high-valence (Mn^{4+} or Mn^{3+}) and low-valence (Mn^{3+} or Mn^{2+}) cations , Ti doping can increase the amount of Mn^{3+} and probably Mn^{4+}, thus increase its electric conductivity; ⅳ)the lattice shrinking of Li_2MnSiO_4 during charging is minimized by the support of unchangeable radius of Ti^{4+} to stabilize the structure.

Fig.6 demonstrates the rate capabilities of pristine Li_2MnSiO_4 and Ti-doped $Li_2Mn_{1-x}Ti_xSiO_4$(x=0.06, 0.1 and 0.2) samples. The charge-discharge current densities are various from 0.03C to 2C (1C=330 mA g^{-1}). It is surprising to note that Ti-doped $Li_2Mn_{1-x}Ti_xSiO_4$ samples exhibit superior rate capability, as shown in the Fig.6. At 1C-rate, the discharge capacities of Ti-doped samples in the second cycle are 114, 120, 76 mAh g^{-1} for 0.06Ti, 0.1Ti, 0.2Ti, respectively. Even at higher rate (2C), the Ti-doped samples still keep the discharge capacity of around 70 mAh g^{-1}, whereas the undoped sample almost loses the ability to discharge. The excellent rate capabilities of Ti-doped samples should be ascribed to the enhancement of electronic conductivity and migration rate of Li ions, which can be further confirmed by the results of electrochemical impedance spectra in the following section.
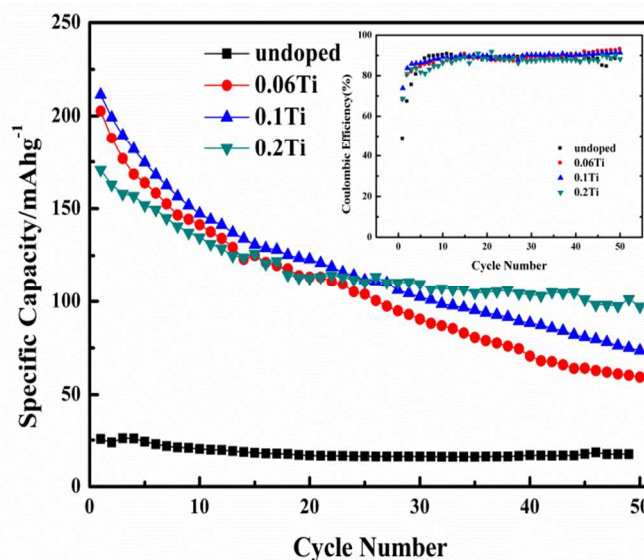
Fig.5 Cycling performance of $Li_2Mn_{1-x}Ti_xSiO_4$(x=0, 0.06, 0.1 and 0.2) electrodes in the voltage range of 1.5-4.8V under the current density of 10 mA g^{-1} at 30℃
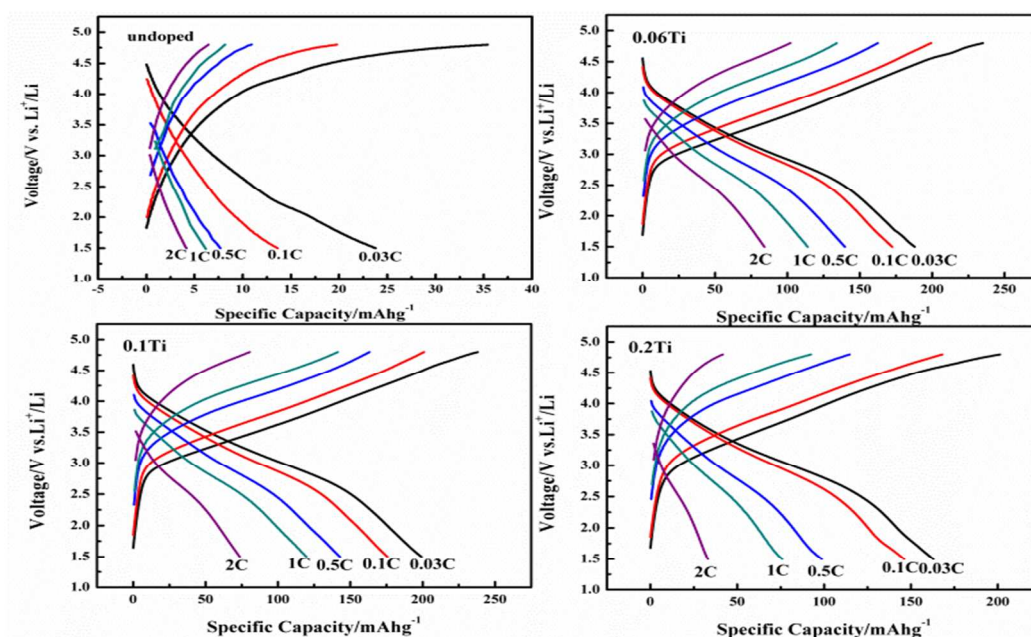
Fig.6 Charge-discharge curves of $Li_2Mn_{1-x}Ti_xSiO_4$(x=0, 0.06, 0.1 and 0.2) electrodes with various current densities at 30 °C (1C=330mA g^{-1})

Electrochemical impedance spectra (EIS) are employed to characterize the kinetic properties of pristine Li_2MnSiO_4 and $Li_2Mn_{1-x}Ti_xSiO_4$(x=0.06, 0.1 and 0.2) samples. Fig.7a demonstrates the Nyqvist plots of the impedance spectra for all samples, and the equivalent circuit mode in the inset of

Fig.7a is used for fitting the impedance data. All spectrums are consisted of a depressed small semicircle in the high-frequency region, a large semicircle in the middle-frequency and a slightly inclined line in the low-frequency region. The semicircles represent the solution resistances (R_s), film
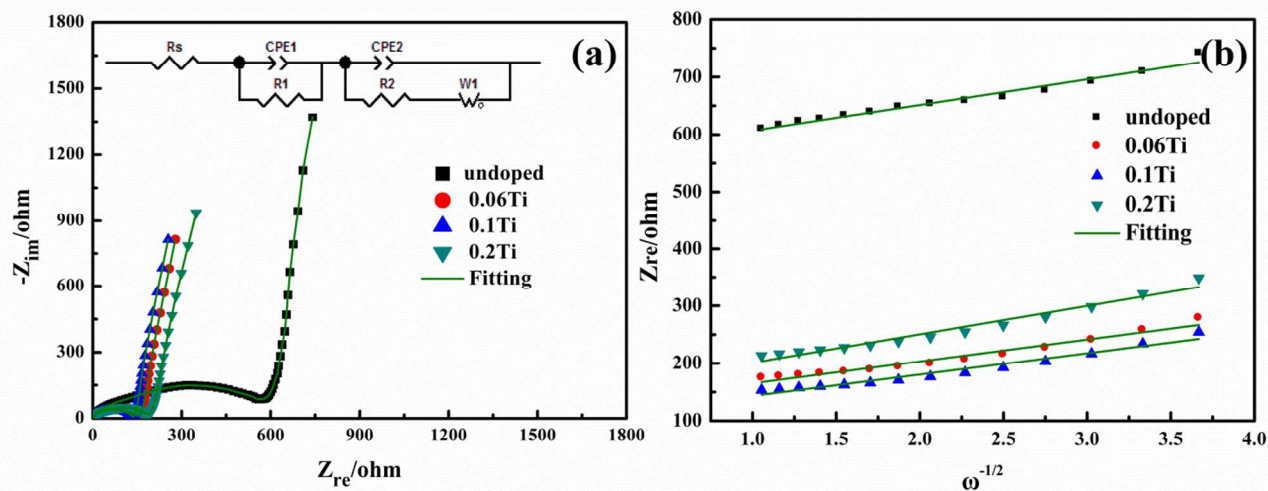
Fig.7 Electrochemical impedance spectra of $Li_2Mn_{1-x}Ti_xSiO_4$(x=0, 0.06, 0.1 and 0.2) electrodes

Table 3 The fitting impedance parameters of as-prepared $Li_2Mn_{1-x}Ti_xSiO_4$(x=0, 0.06, 0.1 and 0.2) samples

	Rs/ohm	R_1/ohm	R_2/ohm	D_{Li}^+/cm^{2}s^{-1}
Li_2MnSiO_4	1.923	100.2	433.6	2.3×10^{-15}
$Li_2Mn_{0.94}Ti_{0.06}SiO_4$	1.727	55.6	81.14	3.2×10^{-15}
$Li_2Mn_{0.9}Ti_{0.1}SiO_4$	3.82	57.69	68.3	3.3×10^{-15}
$Li_2Mn_{0.8}Ti_{0.2}SiO_4$	1.733	81.14	88.65	1.9×10^{-15}

Resistances (R_1) and charge transfer resistance (R_2), respectively. The inclined lines are attributed to the Li ions diffusion in the electrode bulks, which are called Warburg diffusion (Z_w).[28-31] The obtained fitting parameters are displayed in Table 3. It is seen that almost all of the resistances of Ti-doped $Li_2Mn_{1-x}Ti_xSiO_4$ are smaller than that of undoped Li_2MnSiO_4, especially charge transfer resistance (R_2). The values of charge transfer resistance are 81.14, 68.3, 88.65 Ω for 0.06Ti, 0.1Ti, 0.2Ti samples, respectively, much smaller than that of undoped sample (433.6 Ω). The lower R_2 of Ti-doped samples indicates that Ti doping facilitates the charge transfer at the interface, leading to high capacity and superior rate capability as observed. Besides, the diffusion coefficients of Li^+ in the electrodes can be calculated based on the following equation：

$$D_{Li^+} = (R^2T^2)/(2A^2n^4F^4C^2\sigma_w{}^2) \tag{1}$$

Where, R is gas constant, T is the absolute temperature, A is the electrode area, n is the transfer electron, F is the Faraday's constant, C is the molar concentration of Li^+ and σ_w is the Warburg coefficient which can be obtained by following equation:[32,33]

$$Z_{re} \propto \sigma_w\omega^{-1/2} \tag{2}$$

Where, ω is the angular frequency in the low frequency region. As shown in Table 3, the calculated values of Li^+ diffusion coefficients are 2.3×10^{-15}, 3.2×10^{-15}, 3.3×10^{-15}, 1.9×10^{-15} cm^2s^{-1} for undoped, 0.06Ti, 0.1Ti, 0.2Ti samples, respectively. We observe from the results that the Li^+ diffusion coefficients do not present an obvious increasing tendency with the increasing of Ti content. For 0.06Ti and 0.1Ti samples, the Li^+ diffusion coefficients have a little improvement, indicating that Li^+ can easily migrate to the active materials so as to enhance ionic conductivity. However, for 0.2Ti sample, the value has a slight decline. This might be ascribed to impurities existed in the powder which block the lithium ion mobility. Therefore, we can conclude that the content of doping elements is not the much, the better. Moderate substitution of Mn with supervalent cation Ti is beneficial to improve the electronic and ionic conductivity of Li_2MnSiO_4 material to enhance the electrochemical performance.

Conclusions

In summary, we successfully prepared pristine Li_2MnSiO_4 and Ti-doped $Li_2Mn_{1-x}Ti_xSiO_4$(x=0.06, 0.1 and 0.2) powders by a facile sol-gel method. XRD measurements confirm the structures of all the as-prepared powders are in agreement with orthorhombic $Pmn2_1$ space group. FE-SEM images and BET specific surface areas demonstrate that Ti-doped $Li_2Mn_{1-x}Ti_xSiO_4$(x=0.06, 0.1 and 0.2) samples possess smaller particle sizes, better monodispersion and larger specific surface areas, as compared to those of pristine Li_2MnSiO_4. Ti-doped $Li_2Mn_{1-x}Ti_xSiO_4$ electrodes exhibit dramatically increased capacity of 298, 286, 248 mAh g^{-1} for first charging and 203, 211, 171

mAh g^{-1} for first discharging, respectively, much higher than that of pristine sample. Among these Ti-doped materials, $Li_2Mn_{0.8}Ti_{0.2}SiO_4$ shows the best cycling performance, maintaining the capacity around 100 mAh g^{-1} after 50 cycles. Moreover, Ti-doped samples also present superior rate capability. At 1C rate, they have the discharge capacities of 114, 120, 76 mAh g^{-1} for 0.06Ti, 0.1Ti, 0.2Ti samples, respectively. Even at higher rate (2C), the Ti-doped samples still keep the discharge capacity of around 70 mAh g^{-1}. The remarkable enhancement of battery performance in terms of capacity and rate capability for Ti-doped $Li_2Mn_{1-x}Ti_xSiO_4$ is primarily attributed to the decrease of charge transfer resistance and the improvement of Li^+ mobility coefficient. Nevertheless, we don't clearly understand the mechanism of defects formation about aliovalent doping at present, the results indeed demonstrate a new strategy for conductivity enhancement and the possible structural stabilization which may lead to excellent electrochemical properties of Li_2MnSiO_4 cathode materials.

Acknowledgements

Notes and references

a College of Materials Science and Engineering, Nanjing Tech University, Nanjing 210009,China. Fax: +86 25 83240205; Tel: +86 25 83587240; E-mail: maliqun@njtech.edu.cn (L. Ma), yangmengyy@njtech.edu.cn (M. Yang)

1. R. Dominko, M. Bele, and A. Kokalj, Journal of Powder Sources, 2007, 174, 457-461
2. R. J. Gummow, N. Sharma and V. K. Peterson, Journal of Solid State Chemistry, 2012, 188, 32
3. K. Karthikeyan, V. Aravindan and S. B. Lee, Journal of Power Source, 2010, 195, 3761
4. M. S. Islam, R. Dominko and C. Masquelier, Journal of Materials Chemistry, 2011, 21, 9811
5. M. K. Devaraju, T. Tomai and A. Unemoto, RSC Adv., 2013, 3, 608.
6. Y. X. Li, Z. L. Gong and Y. Yang, Journal of Power Sources, 2007, 174, 528
7. S. Zhang, Y. Li and G. J. Xu, Journal of Power Sources, 2012, 213, 10
8. I. Belharouak, A. Abouimrane and K.Amine, Journal of Physical Chemistry, 2009, 113, 20733
9. W. G. Liu, Y. H. Xu and R. Yang, Journal of Alloys and Compounds, 2009, 480, L1
10. S. Zhang, Z. Lin and L. W. Ji, Journal of Materials Chemistry, 2012, 22, 14661
11. S. H. Choi, S. J. Kim and Y. J. Yun, Material Letters, 2013, 105, 113
12. N. Kuganathan, M. S. Islam, Chemistry Materials, 2009, 21, 5196
13. C. Deng, S. Zhang and Y. X. Wu, Journal of Electroanalytical Chemistry, 2014, 719, 150
14. C. Deng, S. Zhang and S. Y. Yang, Journal of Powder Sources, 2011, 196, 386

15 S. H. Wang, J. Yang and X. B. Wu, Journal of Power Sources, 2014, 245, 570

16 D. M. Kempaiah, D. Rangappa, and I. Honma, Chemical Communications, 2012, 48, 2698

17 I. B. ouak, A. Abouimrane and K. Amine, Journal of Physics Chemistry C, 2009, 113, 20733

18 H. Y. Wang, T. L. Hou and D. Sun, Journal of Power Sources, 2014, 247, 497

19 V. Aravindan, K. Karthikeyan and S. Amaresh, Ionics, 2011, 17, 3

20 C. Deng, Y. H. Sun and S. Zhang, International Journal of Electrochemical Science, 2012, 7, 4559

21 R. Y. Chen, R. Heinzmann and S. Mangold, Journal of Physics Chemistry, 2011, 117, 884

22 B. B. Tian, H. F. Xiang and L. Zhang, Electrochimica Acta, 2010, 5, 5453

23 L. Y. Bao, W. Gao and Y. F. Su, Chinese Science Bulletin, 2013, 58, 575

24 M. E. Arroyo-deDompablo, R. Dominko and J. M. Gallardo-Amores, Journal of Chemistry Materials, 2008, 20, 5574

25 V. Aravindan, S. Ravi and W.S. Kim, Journal of Colloid and Interface Science, 2011, 355, 472

26 V. Aravindan, K. Karthikeyan and S. Amaresh, Electrochemical and Solid-State Letters, 2011, 14, A33

27 Q. Q. Zhang, Q. C. Zhuang and S. D. Xu, Ionics, 2012, 18, 487

28 C. L. Tan, H. J. Zhou and W. S. Li, Journal of Power Sources, 2008, 184, 408

29 A. Bhaskar, M. Deepa and T. N. Rao, Journal of the Electrochemical Society, 2012, 159, A1954

30 Z. Z. Feng, J. Yang and Y. N. Nuli, Journal of Power Sources, 2008, 184, 604

31 C. Deng, S. Zhang and B. L. Fu, Materials Chemistry and Physics, 2010, 120, 14

32 M. Yang, X. Y. Zhao and Y. J. Bian, Journal of Materials Chemistry, 2012, 22, 6200

33 S. K. Liu, J. Xu and D. Z. Li, Journal of Power Sources, 2013, 232, 258